

## Progressive aridification in East Africa over the last half million years and implications for human evolution

R. Bernhart Owen, Veronica Muiruri, Tim Lowenstein, Robin Renaut, Nathan Rabideaux, Shangde Luo, Alan Deino, Mark Sier, Guillaume Dupont-Nivet, Emma McNulty, et al.

### ► To cite this version:

R. Bernhart Owen, Veronica Muiruri, Tim Lowenstein, Robin Renaut, Nathan Rabideaux, et al.. Progressive aridification in East Africa over the last half million years and implications for human evolution. *Proceedings of the National Academy of Sciences of the United States of America*, National Academy of Sciences, 2018, 115 (44), pp.11174-11179. 10.1073/pnas.1801357115 . insu-01895379

**HAL Id: insu-01895379**

**<https://hal-insu.archives-ouvertes.fr/insu-01895379>**

Submitted on 15 Oct 2018

**HAL** is a multi-disciplinary open access archive for the deposit and dissemination of scientific research documents, whether they are published or not. The documents may come from teaching and research institutions in France or abroad, or from public or private research centers.

L'archive ouverte pluridisciplinaire **HAL**, est destinée au dépôt et à la diffusion de documents scientifiques de niveau recherche, publiés ou non, émanant des établissements d'enseignement et de recherche français ou étrangers, des laboratoires publics ou privés.

# Progressive aridification in East Africa over the last half million years and implications for human evolution

Richard Bernhart Owen<sup>1</sup>, Veronica Muiruri<sup>1</sup>, Tim Lowenstein<sup>2</sup>, Robin Renaut<sup>3</sup>, Nathan Rabideaux<sup>4</sup>, Shangde Luo<sup>5</sup>, Alan Deino<sup>6</sup>, Mark Sier<sup>7</sup>, Guillaume Dupont-Nivet<sup>8</sup>, Emma McNulty<sup>2</sup>, Kennie Leet<sup>2</sup>, Andrew Cohen<sup>9</sup>, Christopher Campisano<sup>10</sup>, Daniel Deocampo<sup>4</sup>, Chuan-Chou Shen<sup>11</sup>, Anne Billingsley<sup>9</sup>, Anthony Mbuthia<sup>12</sup>

<sup>1</sup>Hong Kong Baptist University, <sup>2</sup>Binghamton University, <sup>3</sup>University of Saskatchewan, <sup>4</sup>Georgia State University, <sup>5</sup>National Cheng-Kung University, <sup>6</sup>Berkeley Geochronology Center, <sup>7</sup>University of Oxford, <sup>8</sup>French National Centre for Scientific Research, <sup>9</sup>University of Arizona, <sup>10</sup>Arizona State University, <sup>11</sup>National Taiwan University, <sup>12</sup>Tata Chemicals

Submitted to Proceedings of the National Academy of Sciences of the United States of America

**Evidence for Quaternary climate change in East Africa has been derived from outcrops on land, lake cores and from marine dust, leaf wax and pollen records. These data have previously been used to evaluate the impact of climate change on hominin evolution, but correlations have proven to be difficult given poor data continuity and the great distances between marine cores and terrestrial basins where fossil evidence is located. Here we present the first continental coring evidence for progressive aridification since about 575 thousand years ago (ka), based on Lake Magadi (Kenya) sediments. This long-term drying trend was interrupted by many wet-dry cycles, with the greatest variability developing during times of high eccentricity-modulated precession. Intense aridification apparent in the Magadi record took place between 525–400 ka, with relatively persistent arid conditions after 350 ka and through to the present. Arid conditions in the Magadi Basin coincide with the Mid-Brunhes Event and overlap with mammalian extinctions in the South Kenya Rift between 500–400 ka. The 525–400 ka arid phase developed in the South Kenya Rift between the period when the last Acheulean tools are reported at about 500 ka and prior to the appearance of Middle Stone Age artefacts by about 320 ka. Our data suggest that increasing mid-late Pleistocene aridification and environmental variability may have been drivers in the physical and cultural evolution of *H. sapiens* in East Africa.**

Quaternary | paleoclimate | paleolimnology | hominins | Lake Magadi

Several hypotheses have attempted to explain human evolution and its possible relationship with environmental change (1, 2). The savannah hypothesis suggested that bipedalism resulted from hominins moving from forests to grassy savannas (3). Other theories emphasized climate as an evolution driver, including the aridity, turnover pulse, variability selection and accumulated plasticity hypotheses (4–7). Evaluation of these ideas has been hindered by a lack of basin-scale records that can provide a high-resolution environmental context. The Hominin Sites and Paleolakes Drilling Project (HSPDP) has attempted to fill this gap by providing continental sedimentary records that can be linked to nearby hominin fossils and artefacts in Ethiopia and Kenya (8).

Here we present evidence from the southernmost HSPDP site, at Lake Magadi (Fig. 1), that is relevant to debates about the climatic context of human evolution, from an area close to some of the most important records of hominin prehistory. The Lake Magadi record spans the past one million years (Fig. 2; see SI Appendix text, Figs. S1–3 and Tables S1–7 for details of dating methods) and can be compared with --a 1.2 million-year (Ma) sequence at Olorgesailie, 25 km to the northeast (9–11). The Olorgesailie deposits and archeological record document a transition from Acheulean to Middle Stone Age (MSA) toolkits (12–14), with the Magadi core, and cores from the neighboring Koora Basin drilled by the Olorgesailie Drilling Project (8, 15), covering the period when *H. sapiens* emerged in Africa (16). The

Magadi and Olorgesailie records also span a turnover in large mammals before 320 ka (14), which has also been documented at Lainyamok between 500–400 ka, 15 km west of Magadi (17). Thus, Lake Magadi is located in a region containing archeological and paleontological Middle Pleistocene sites that provide critical information about the relationships between climate dynamics and human prehistory.

Lake Magadi is a seasonally flooded saline alkaline pan about 606 m above sea level in the South Kenya Rift (Fig. 1a) surrounded by poorly correlated cherts, silts and evaporites (18–19). Core HSPDP-MAG14-2A (hereafter MAG14-2A, Fig. 1b) includes trona, zeolitic mud, chert, tuff, and carbonate grainstone deposited in a regional tectonic sump that has been occupied by a lake since eruption of the underlying lavas (1.08 Ma). This study combines geochemical, mineralogical, diatom and pollen analyses that indicate a trend towards a more saline, alkaline lake and a more arid climate from about 575 ka to the present. This progressive change was interrupted by wetter episodes, but was directional in overall character towards increasing aridity.

## Results

**Progressive changes in geochemistry and mineralogy.** Loss on Ignition (LOI) at 1,000°C (Fig. 2a; SI Appendix, Table S7) indicates combustible carbonates (calcite, trona) and organic matter. High LOI values before 950 ka, or 187 meters below surface (mbs), reflect shallow water carbonate grainstones. LOI (550°C) is low (<3%) between 950–800 ka (187–178 mbs) with higher val-

## Significance

Previous research hypotheses have related hominin evolution to climate change. However, most theories lack basin-scale evidence for a link between environment and hominin evolution. This study documents continental, core-based, evidence for a progressive increase in aridity since about 575 ka in the Magadi Basin with a significant change from the Mid-Brunhes Event (~ 430 ka). Intense aridification in the Magadi Basin corresponds with faunal extinctions and changes in toolkits in the nearby Olorgesailie Basin. Our data are consistent with climate variability as an important driver in hominin evolution, but also suggest that intensifying aridity may have had a significant influence on the origins of modern *H. sapiens* and the onset of the Middle Stone Age.

## Reserved for Publication Footnotes

137  
138  
139  
140  
141  
142  
143  
144  
145  
146  
147  
148  
149  
150  
151  
152  
153  
154  
155  
156  
157  
158  
159  
160  
161  
162  
163  
164  
165  
166  
167  
168  
169  
170  
171  
172  
173  
174  
175  
176  
177  
178  
179  
180  
181  
182  
183  
184  
185  
186  
187  
188  
189  
190  
191  
192  
193  
194  
195  
196  
197  
198  
199  
200  
201  
202  
203  
204

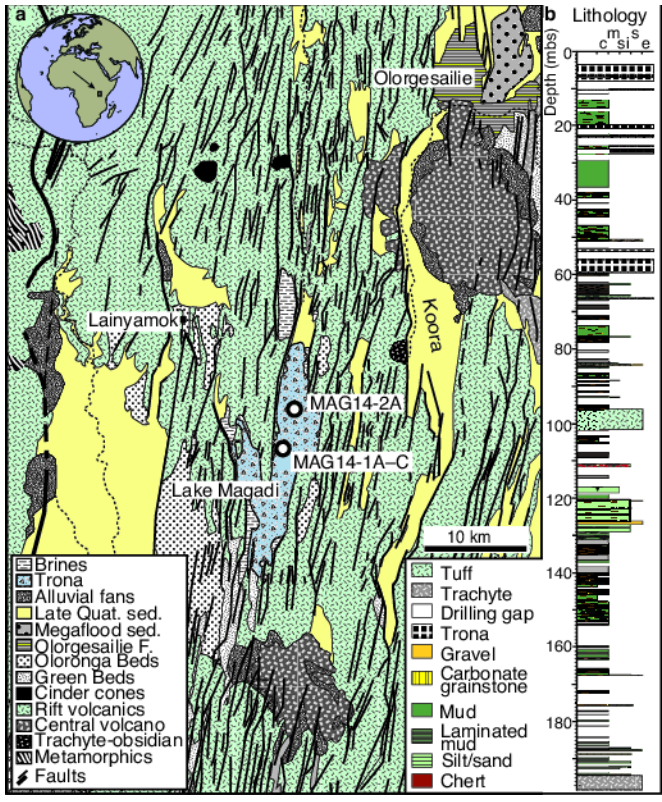


**Fig. 1. Core location and lithology.** a, Location of MAG14-2A and 1A and geology. b, Sediment log for MAG14-2A; c=clay, m = mud, si = silt, s = sand, e = evaporites.

ues (5–20%) in younger sediments suggesting greater lake floor anoxia. Major increases in LOI in sediments <111 ka (65 mbs) reflect increases in organics and trona, which accumulated in highly saline alkaline, anoxic waters. Na/Ca ratios increased with time (Fig. 2a) as a result of a shift from calcium-rich (calcite, Mg-calcite) to Na- and K-rich (erionite, trona) chemical sediments. The upward decline in Ca probably reflects early precipitation of CaCO<sub>3</sub> near shorelines where streams entered an alkaline paleolake and relative increases in groundwater contributions, as drier conditions developed, which would have favored lower Ca through subsurface precipitation.

Mineralogical data also document progressive changes (Fig. 2a). Authigenic minerals are dominated by calcite and Mg-calcite in sediments >385 ka (103 mbs), indicating fresh to mildly saline groundwater. Analcime occurs throughout the core with other zeolites accumulating since 375 ka, indicating a shift towards more saline alkaline conditions. The zeolites formed from Na-Al-Si alkaline spring gels washed into the basin or by alteration of aluminosilicate minerals or volcanic glass (20). Trona was deposited after 111 ka (65 mbs) in highly saline, alkaline water.

**Diatom and pollen stratigraphy.** Diatoms are absent in MAG14-2A sediments >545 ka (132 mbs), but are present in basal limestones in a second core, MAG14-1A (Fig. 1a), where benthic and epiphytic taxa indicate freshwater swamps. A few cherts contain *Anomoeoneis sphaerophora*, a moderate to high salinity taxon present in shallow springs today (21). The occurrence of diatoms only in well-cemented chert and limestone suggests they may have dissolved from unlithified deposits. The dominant taxa in the diatomaceous interval (about 545–16 ka; 132–38 mbs) include mixed planktonic freshwater (*Aulacoseira granulata*, *A. agassizi*) and saline species (*Cyclotella meneghiniana*, *Thalassiosira faurii*; details in SI Appendix, Fig. S4 and Dataset S1), suggesting a deep meromictic lake with permanent saline

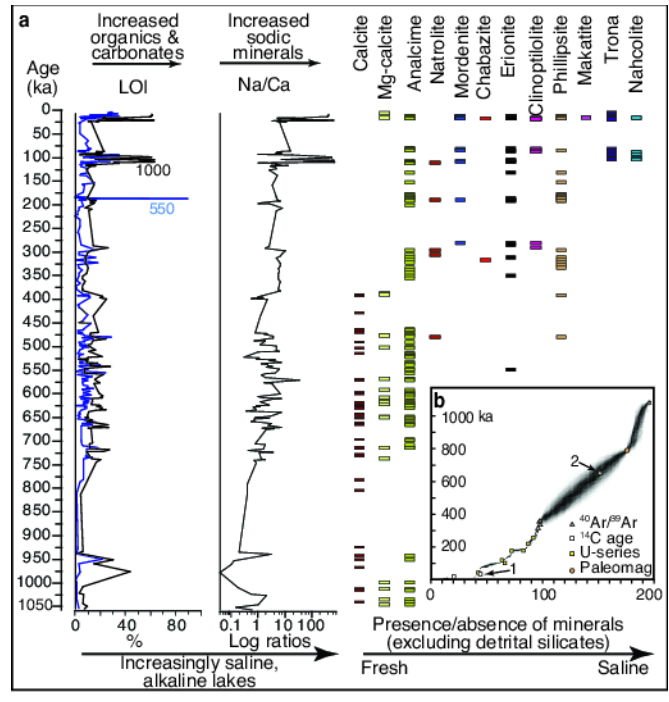


**Fig. 2. Core chronology, geochemistry and mineralogy.** a, Geochemistry and mineralogy. LOI (550/1000) = Loss on Ignition and ignition temperatures (centigrade). Profile of Na/Ca ratios. Major authigenic minerals (excluding clays, quartz, feldspar) determined by X-ray diffraction. Minerals ordered to reflect generally higher salinities to the right. b, Bayesian chronological model. 1 = Excluded <sup>14</sup>C date that fails to follow a monotonic ordering. 2 = Excluded <sup>40</sup>Ar/<sup>39</sup>Ar date from a single crystal. Two chert dates from samples later found to contain secondary chalcidony were also excluded from the model. See SI for details.

waters that were periodically overtopped by fresh fluvial inputs. The evidence for flooding is supported by intermittent freshwater benthic taxa (22) such as *Cocconeis placentula*, *Encyonema muelleri* and *Epithemia* spp.

Mean transfer functions for all diatoms indicate pH of about 7.4–11.4 and conductivities of 300–40,000 μS cm<sup>-1</sup> (Fig. 3). However, given the evidence for episodic meromixis, there is a need to recalculate the data separately for surface freshwater and deeper saline water taxa (Fig. 3), which suggests that the pH of freshwater inputs ranged between 7.3–8.5 with conductivities of 200–2,000 μS cm<sup>-1</sup>. The saline floras document increased pH after about 385 ka (103 mbs), from 9.2–10 to 9.4–11.5. An absence of diatoms after about 18 ka suggests that pH and conductivity exceeded tolerance limits or resulted in dissolution.

Grasses (Poaceae) dominated with a smaller sedge (Cyperaceae) component before about 900 ka (184 mbs), with pollen not preserved between 900–735 ka (184–168 mbs) (Fig. 4; detailed floras in SI Appendix, Figs. S9–S10 and Dataset S2), possibly due to oxygenated conditions. Cyperaceae increased relative to Poaceae between about 735–520 ka (168–127 mbs) and dominated between 605–568 ka (143–136 mbs), with other minor aquatics (*Typha*, *Potamogeton*), suggesting shallow fresh waters (21). There were also significant increases in *Podocarpus* (735–520 ka) and *Olea* (698–635 ka; 160–147 mbs) with *Juniperus* appearing after 735 ka. *Podocarpus* is common in modern upland forests in Kenya and, where abundant, has been used to infer expansion of Afromontane forests or changes in fluvially-transported regional pollen (23, 24). The parallel trends for *Podocarpus*, Cyperaceae and the other aquatic indicators imply a climatic control. Although broadly the wettest interval in the last million years, climate varied with a drier episode at about 662–625

205  
206  
207  
208  
209  
210  
211  
212  
213  
214  
215  
216  
217  
218  
219  
220  
221  
222  
223  
224  
225  
226  
227  
228  
229  
230  
231  
232  
233  
234  
235  
236  
237  
238  
239  
240  
241  
242  
243  
244  
245  
246  
247  
248  
249  
250  
251  
252  
253  
254  
255  
256  
257  
258  
259  
260  
261  
262  
263  
264  
265  
266  
267  
268  
269  
270  
271  
272



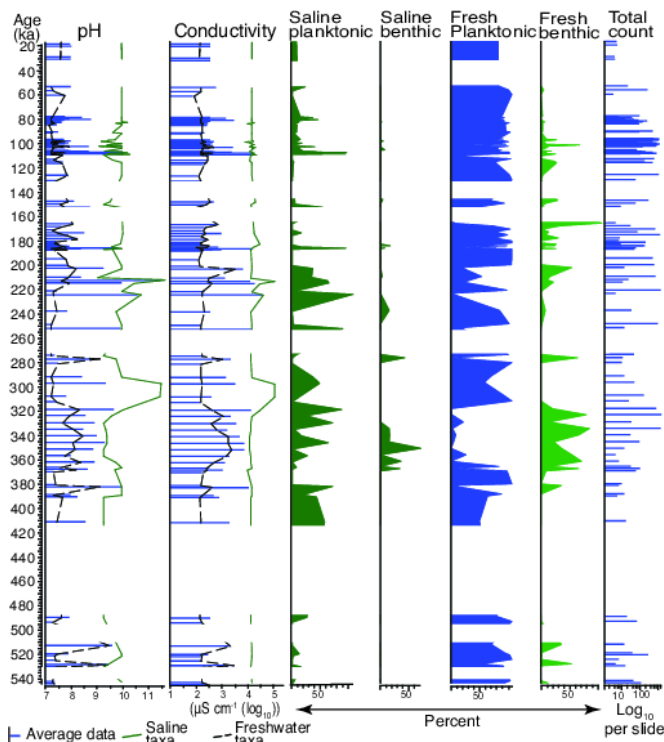


**Fig. 3. Diatom-based environmental data.** Diatoms accumulated in a meromictic lake so separate conductivity and pH transfer functions are shown for mixed, saline and fresh water taxa. Habitats indicated separately for saline and fresh taxa.

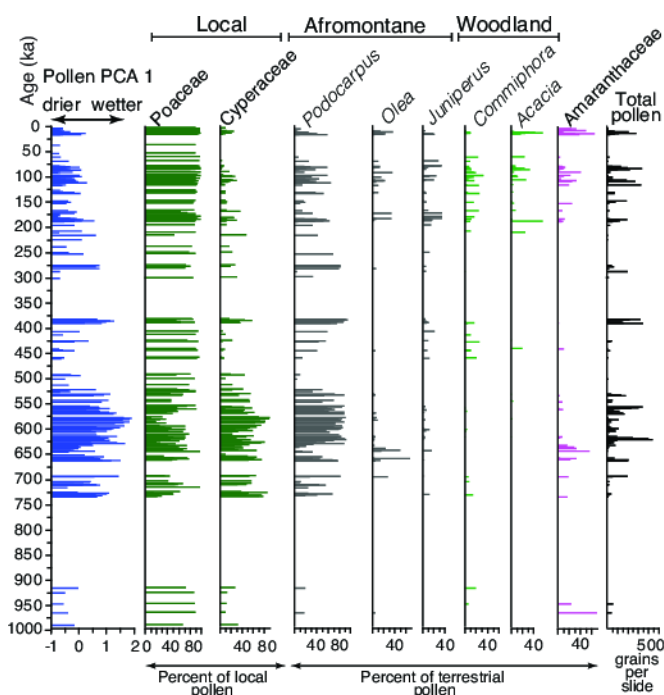


**Fig. 4. Pollen stratigraphy.** Selected taxa shown. Pollen PCA 1 summarizes all pollen data and shows a long-term reduction in PCA values from ~575 ka that reflects increased aridity. Poaceae increase upwards with Cyperaceae and *Podocarpus* declining. Other taxa suggest increasing aridity during the last half million years.

ka (153–146 mbs) marked by increased *Amaranthaceae*, with the wettest conditions at 575 ka (137 mbs) (Fig. 4).

Cyperaceae and *Podocarpus* declined between about 520–400 ka (127–105 mbs), suggesting greater aridity at a time when diatoms indicate a meromictic lake and/or alternating saline and freshwater lakes. A recovery in *Podocarpus* and Cyperaceae between 400–275 ka (105–94 mbs) suggests a wetter interval that was followed by a decline in these taxa. During the last 275 ka (94 mbs) a variety of taxa expanded and contracted, reflecting wetter and drier settings, but with an overall trend towards greater aridity. *Olea*, for example, is derived from wet and dry upland evergreen forests and varies in abundance between about 275–5 ka (94–7 mbs) when it disappears. *Commiphora* and *Acacia* increase after 205 ka (87 mbs) suggesting dry semi-deciduous dense bushland, with drought-related *Amaranthaceae* and *Juniperus*, associated with drier upland forests (25), also common. Increases in Cyperaceae along with herbaceous pollen such as *Hydrocotyle* between about 12–8 ka (17–12 mbs) suggest fresher waters. Afromontane and woodland species were replaced by herbaceous pollen and Poaceae through the last 8 ka with Poaceae forming nearly 100% of the flora after 4 ka (6 mbs).

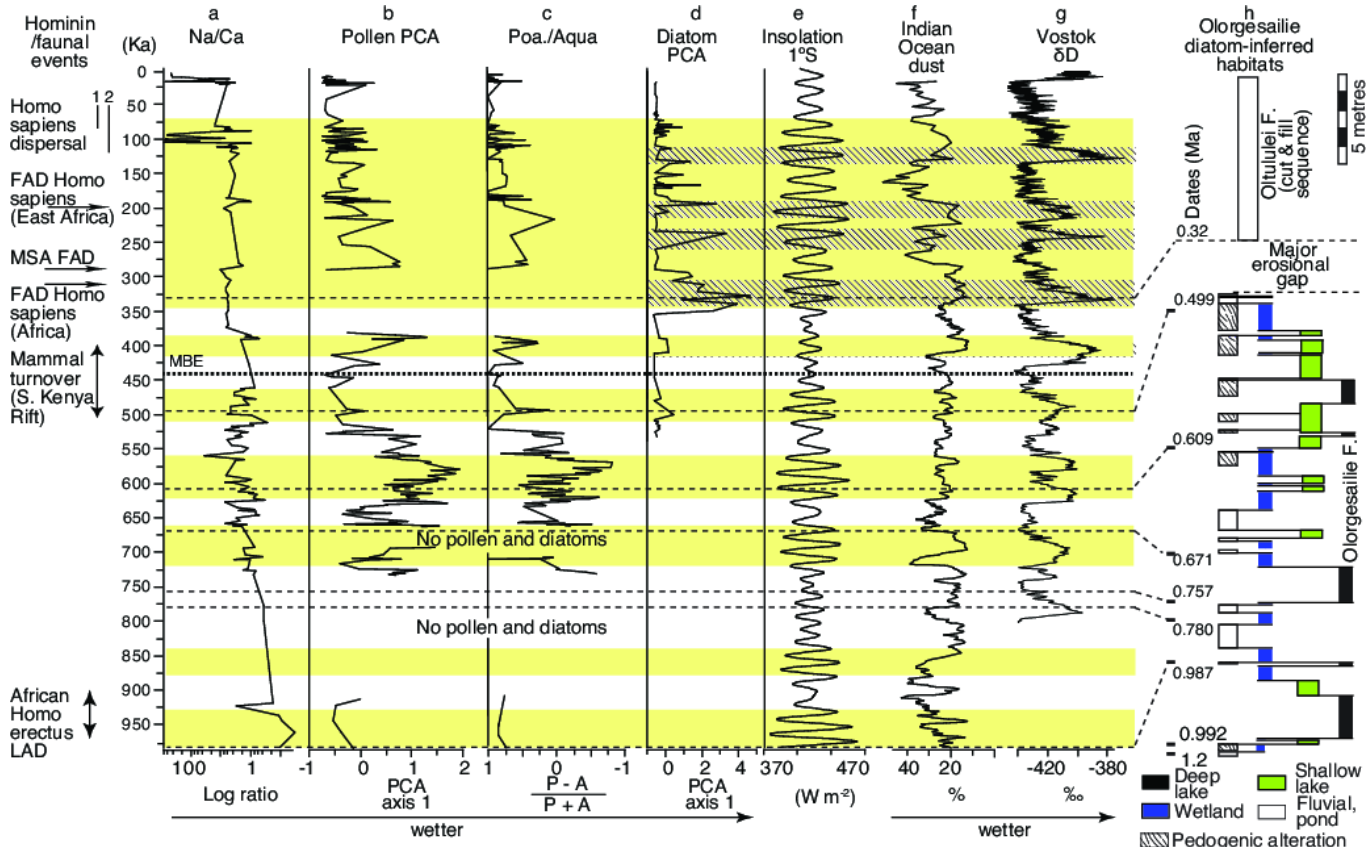
Na/Ca ratios, PCA data for all pollen, and grass to aquatic pollen ratios indicate an overall progressive change during the last half million years (Fig. 5). Prior to 575 ka the basin had trended towards wetter conditions, but then there was an overarching shift towards greater aridity superimposed on multiple wet-dry cycles. Independent terrestrial and aquatic datasets that varied in unison indicate that this change was not simply due to lake hydrology and local tectonics, but was driven by a directional climate shift. Intermittent positive spikes in diatom PCA data between 350–70 ka reflect increases in shallow, freshwater, diatoms. The strong contrast in habitat preferences between the dominant mixed saline and fresh, deep-water planktonic taxa (*Thalassiosira* spp., *Aulacoseira granulata* and variety *valida*) and episodic shallow, freshwater, lake/wetland (*A. agassizi*, *A. granulata* v. *angustissima*) and benthic floras (Fig. 3) suggest that the latter may have been transported intermittently by floods from nearby swampy and/or fluvial settings to the core site (22). Many of the younger spikes also match pollen evidence for wetter periods (195, 170, 125, 95, 80 ka) and interglacial episodes. The amplitude of the spikes decrease with time, as does their temporal spacing. A lack of diatoms after about 16 ka reflects the formation of an ephemeral hypersaline playa.

## Discussion

**Climate change.** On a global scale a major inflection point in Pleistocene climate, the Mid-Brunhes Event (MBE), close to the boundary between Marine Oxygen Isotope stages 12 to 11, took place about 430 ka. Subsequently, there was increased climate variability with the development of colder glacial periods and warmer interglacial episodes (26, 27), although it has been suggested that the MBE is regionally inconsistent. Terrestrial data from the UK (28), for example, have been used to infer no significant change across the MBE, whereas continental evidence from Spain (29) supports a climate transition.

The continental pollen record from equatorial Lake Magadi provides strong support for a climate transition at the MBE (Fig. 5), suggesting a potential link to global CO<sub>2</sub>/glacial cyclicity, with a major change from wetter conditions to greater aridity after about 430 ka. The overall trend towards dryer conditions was initiated about 575 ka, with particularly intense aridity developing between 525–400 ka, which partially overlaps with Marine Oxygen Isotope Stage 11 (424–374 ka), the warmest interglacial of the last 500 ka (30). Subsequently, many wetter and drier cycles were superimposed on progressive aridification, with diatomaceous parts of the core documenting a tendency towards increased flood inputs of benthic taxa (increased PCA values) during interglacial episodes (Fig. 5).

409  
410  
411  
412  
413  
414  
415  
416  
417  
418  
419  
420  
421  
422  
423  
424  
425  
426  
427  
428  
429  
430  
431  
432  
433  
434  
435  
436  
437  
438  
439  
440  
441  
442  
443  
444  
445  
446  
447  
448  
449  
450  
451  
452  
453  
454  
455  
456  
457  
458  
459  
460  
461  
462  
463  
464  
465  
466  
467  
468  
469  
470  
471  
472  
473  
474  
475  
476



477  
478  
479  
480  
481  
482  
483  
484  
485  
486  
487  
488  
489  
490  
491  
492  
493  
494  
495  
496  
497  
498  
499  
500  
501  
502  
503  
504  
505  
506  
507  
508  
509  
510  
511  
512  
513  
514  
515  
516  
517  
518  
519  
520  
521  
522  
523  
524  
525  
526  
527  
528  
529  
530  
531  
532  
533  
534  
535  
536  
537  
538  
539  
540  
541  
542  
543  
544

**Fig. 5. Temporal environmental change in the Magadi basin and regional comparisons.** Major hominin/faunal events in eastern Africa (except where noted) to left (8). First appearance of *H. sapiens* in Africa from Morocco data (16). *H. sapiens* dispersal: 1 = genetic data (41), 2 = fossil data (39, 40). FAD = First Appearance Datum; LAD = Last Appearance Datum. Thick dashed line shows the Mid-Brunhes Event (MBE). a, Na/Ca ratios. Decline reflects change from fresh to saline alkaline lake. b, Pollen PCA 1. Low values reflect increased aridity. c, Poaceae to aquatic pollen ratios (P-A/P+A). High values indicate wetter episodes. d, Diatom Principal Component Analysis. High values reflect benthic taxa introduced to a meromictic lake by flooding. Note that many of these flood events broadly correlate (diagonal shading) with interglacial episodes in "g". e, Insolation (1°S) from AnalySeries 2.0. High variability periods shaded. f, Northwest Indian Ocean dust record (26). Note long-term increasing aridity through the last 400 ka. g, Change in deuterium in Vostok ice core, East Antarctica (27). Note increased variability in glacial-interglacial cycles after the MBE. h, Diatom-inferred environmental change, Ologresailie Basin (47).

This directional increase in aridity since ~575 ka has not previously been documented in continuous continental cores from East Africa, although there is support from pedogenic carbonate carbon isotopes in outcrops (31) and eolian dust records from the northwest Indian Ocean (7, 26) (Fig. 5), which suggest a similar pattern of increasing aridity and intermittently wetter intervals through the last half million years. Limited pedogenic carbonate carbon isotope data from Ologresailie indicate an overall increase in C4 grasslands during the last 800 ka (14). Oxygen and carbon isotopes from several sites within a 990 ka Ologresailie Formation paleosol, for example, suggest an abundance of wooded grassland in a cooler and moister environment at that time compared with the modern grassy semi-arid basin (32).

There are also clear correlations for specific intervals in the Magadi record with other African regions. For example, the deposition of iron and intermittent severe reductions in aquatic pollen between about 110–80 ka indicate a series of very dry phases that alternated with wetter intervals. The termination of this drought period lies close to a transition from megadroughts to wetter conditions at Lake Malawi and more widely across tropical Africa (33, 34). However, in contrast, the overall drying trend at Magadi is inconsistent with an inferred shift towards wetter conditions noted at Lake Malawi (35) indicating regional African contrasts in vegetation and climate patterns. However, pollen data (36) show some similarities with high percentages

of *Podocarpus* between 455–325 ka at Malawi coinciding with increased *Podocarpus* at Magadi after 455 Ka.

**Climate and hominin evolution.** The nearby Ologresailie Basin provides detailed information on hominin evolution for the last million years with evidence for a major transition in stone technologies (Fig. 5). The Ologresailie Formation (~1,200–500 ka) includes Acheulean tools (14) whereas MSA artefacts (12) are present in the Oltululei Formation (~320–36 ka) (11), with the transition between these toolkits taking place during a period of erosion at Ologresailie that has been related to faulting and base-level change (10). New environmental data from Magadi show increasing aridity during the period of hiatus at Ologresailie with intense desiccation between 525–400 ka. This suggests that erosion at Ologresailie might partly reflect climatic conditions, with aridity lowering lake and base levels and changing/reducing the vegetation cover, which would, in turn, tend to enhance erosion of more exposed land surfaces (37). Magadi pollen data (SI Appendix, Fig. S5), for example, indicate an expansion of grasslands and reduction in aquatic pollen after about 525 ka. The arid interval also closely overlaps with a major overturn in mammal faunas with local extinction of large-bodied specialized grazing mammals reported from both Ologresailie (14) and Lainyamok (17).

The 525–400 ka dry phase and environmental variability would likely have had a significant impact on contemporary hominin populations regionally. It has been hypothesised (14), for

545 example, that environmental pressures and variability can lead to  
546 an uneven distribution of resources that could drive hominins to  
547 travel more widely and to interact increasingly with other groups  
548 for both raw materials and information. In turn, this would help  
549 to drive technological change and its dissemination, resulting in  
550 increased foraging success rates and ability to survive.

551 The Magadi terrestrial pollen record suggests that the interval  
552 with greatest climate variability took place between about  
553 650–350 ka with moister periods tending to be linked to high-  
554 amplitude insolation variability and with drier episodes develop-  
555 ing at times of low-amplitude insolation (e.g., 655–620, 560–510,  
556 455–410, <75 ka; Fig. 5). Similarly, changes in toolkits overlap  
557 with the 650–350 ka period, with modest reductions in Olorgesailie  
558 Acheulean stone tool sizes reported between 615 and 499  
559 ka (14) and with the smaller toolkits of the MSA developing by  
560 about 320 ka (12–14). This increased environmental variability,  
561 and the intense period of aridity, also overlap with a major  
562 turnover in mammal faunas with several large-bodied specialized  
563 grazing mammals becoming locally extinct and being replaced by  
564 related species with smaller body sizes (14, 17). As the earlier  
565 fauna was already arid-adapted, the progressive increase in aridity  
566 was unlikely to have led to any turnover. However, a change in  
567 variability, that very specialized grazers couldn't adapt to, may  
568 have led to the turnover. It is also possible that increased aridity,  
569 or more variable environmental conditions in the context of  
570 increasing aridity may have impacted hominin populations during  
571 this transitional period by selecting for cognitive abilities to, for  
572 example transport increasingly diversified toolkits over greater  
573 distances, as is evidenced in the nearby Olorgesailie archaeological  
574 record (12).

575 Major steps in Quaternary hominin evolution have also been  
576 linked to eccentricity-modulated high-amplitude insolation cycles  
577 specifically associated with extreme climate variability during  
578 moist intervals, rather than low-amplitude periods when mon-  
579 soons are weakened and climate becomes drier (38). However,  
580 the possible overlap between intense aridity, major changes in  
581 toolkits, and mammal extinctions in the Magadi-Olorgesailie re-  
582 gion argue against this version of a climate-evolution linkage.

583 The period between 350–50 ka represents the longest episode  
584 of eccentricity-modulated high amplitude insolation variability in  
585 the Middle to Late Pleistocene (Fig. 5). This coincides with signif-  
586 icant environmental change when MSA tools emerged, symbolic  
587 cultures developed, *H. sapiens* appeared and the Late Stone Age  
588 commenced (2). Early anatomically modern human fossils from  
589 Asia indicate that they dispersed from Africa between 120–50  
590 ka (39, 40) with genetic data suggesting that ancestral modern  
591 non-African populations originated from Africans that dispersed  
592 between 75–50 ka (41). Gulf of Aden leaf wax isotopes, close to  
593 a possible southern migration route, indicate multiple wet-dry  
594 cycles set against an overall drying trend (42). Our continental  
595 record indicates arid climates that were punctuated by moist  
596 episodes, which may have supported a greener Sahara, opening  
597 the possibility of northern routes.

598 Recent hominin studies have noted that *H. sapiens* and  
599 the cultural materials that they produced may have a polycen-  
600 tric African origin with reproductively semi-isolated populations

601 adapting to local environments alongside genetic drift (43). In  
602 the South Kenya Rift, the 300-ka period of high-amplitude in-  
603 solation variability was characterized by major environmental  
604 and hominin changes, providing support for hypotheses such  
605 as variability selection, which advocates adaptive evolutionary  
606 change during periods of increased environmental variability (4,  
607 38, 44–46). However, it is important to note that this variability  
608 was superimposed on a strongly directional long-term trend to-  
609 wards increased aridity, especially during the critical 525–400 ka  
610 interval of drying documented here, which coincides with major  
611 technological and evolutionary events in the regional human  
612 prehistory. The Magadi record thus suggests that the species and  
613 technological changes in the South Kenya Rift were occurring  
614 against a backdrop of both increased aridity and enhanced vari-  
615 ability, both of which could have acted as strong selective agents  
616 during the transition from the Early to Middle Stone Age and in  
617 the evolution of anatomically modern humans.

## 618 Methods

619 Details of the drilling (June 2014) are presented in the SI Appendix text.  
620 Three holes were drilled at Site 1 with one (MAG14-2A) recovered from Site  
621 2 (Fig. 1a). Core recovery for MAG14-2A was 65% with drilling terminated in  
622 trachyte at ~194mbs.

623 The chronology model (Fig. 2b) made use of one radiocarbon date from  
624 humate fractions of bulk organic matter in the upper core, nine replicate  
625  $^{40}\text{Ar}/^{39}\text{Ar}$  dates from mid core tephra, one  $^{40}\text{Ar}/^{39}\text{Ar}$  date on a basal trachyte  
626 lava and seven U-series dates from chert. An  $^{40}\text{Ar}/^{39}\text{Ar}$  date for a single  
627 feldspar grain from ash at 151 mbs was treated as supplementary and not  
628 included in the model, but plots within the 0.95 probability range for this  
629 depth (see SI Appendix for dating techniques). One  $^{14}\text{C}$  date did not follow a  
630 monotonic sequence and was excluded from the model, but is shown in Fig.  
631 2b. In addition, the model includes the Brunhes-Matuyama boundary in the  
632 lower core.

633 Samples for geochemical (n=343) and LOI (n=332) analyses were col-  
634 lected at about 32 cm intervals and where distinctive lithologies were present  
635 (see SI Appendix for techniques). Diatom samples (n=355) were collected  
636 every 32 cm with additional sampling at 10–15 cm intervals for diatomaceous  
637 sections, yielding 113 samples and 62 diatom taxa between 43–132 m (18–472  
638 ka in SI Appendix, Fig. 54; Datasets S1, S2). A minimum of 400 diatoms  
639 were counted per slide, except where diatoms were rare, in which case  
640 all diatoms were included. Environmental reconstructions are based on the  
641 "Combined Salinity Dataset" in the European Diatom Database (EDDI)  
642 (<http://craticula.ncl.ac.uk/Eddi/jsp/index.jsp>) with taxa matched to the EDDI  
643 classification system. Pollen taxa (n=105) were identified in 354 samples  
644 with common pollen shown in SI Appendix, Figs. S5 and S6 and Datasets  
645 S3 and S4. Pollen and spores were mounted on slides and counted at  
646 400x magnification. Pollen identification was made to the lowest possible  
647 taxonomic level, although some pollen types could only be identified to  
648 family level. The total count per sample generally ranged between 250–500  
649 grains, except in a few samples where preservation was poor.

## 650 Acknowledgments:

651 Funding was provided by the Hong Kong Research Grants Council  
652 (HKBU201912), the International Continental Drilling Program (ICDP), the  
653 U.S. National Science Foundation (EAR-1338553), and the Ministry of Science  
654 and Technology of Taiwan ROC (107L901001, MOST107-2119-M-002-051).  
655 We thank the National Museums of Kenya for support, the National Council  
656 for Science and Technology and the National Environmental Management  
657 Authority of Kenya for permits and Julia Richter for LOI analyses. DOSECC  
658 Exploration Services provided drilling supervision. The Operational Support  
659 Group of ICDP provided downhole logging services. Support was also pro-  
660 vided by LacCore, the National Oil Corporation of Kenya, Tata Chemicals,  
661 the County Government of Kajiado. This is publication number #15 of the  
662 Hominin Sites and Paleolakes Drilling Project.

- 663 1. Potts R (1996) Evolution and climatic variability. *Science* 273:922–923.
- 664 2. Potts R, Faith JT (2015) Alternating high and low climate variability: The context of natural  
665 selection and speciation in Plio-Pleistocene hominin evolution. *J Hum Evol* 87:5–20.
- 666 3. Vrba ES (1994) An hypothesis of heterochrony in response to climatic cooling and its  
667 relevance to early hominid evolution, in *Integrative Paths to the Past*, eds Corruccini R,  
668 Ciochon RL (Prentice Hall), pp 345–376.
- 669 4. Potts R (2013) Hominin evolution in settings of strong environmental variability. *Quat Sci*  
670 *Rev* 73:1–13.
- 671 5. Maslin MA, Brierley CM, Milner AM, Shultz S, Trauth MH, Wilson KE (2014) East African  
672 climate pulses and early human evolution. *Quat Sci Rev* 101:1–17.
- 673 6. Grove M (2014) Evolution and dispersal under climatic instability: a simple evolutionary  
674 algorithm. *Adapt Behav* 22:235–254.

- 675 7. deMenocal PB (1995) Plio-Pleistocene African climate. *Science* 270:53–59.
- 676 8. Campisano CJ, Cohen AS, Arrowsmith JR, Asrat A, Behrensmeier AK, Brown ET, Deino  
677 AL, Deocampo DM, Feibel CS, Kingston JD, Lamb HF, Lowenstein TK, Noren A, Ologo  
678 DO, Owen RB, Pelletier JD, Potts R, Reed KE, Renaut RW, Russell JM, Russell JL,  
679 Schäbitz F, Stone JR, Trauth MH, Wynn JG (2017) The Hominin Sites and Paleolakes  
680 Drilling Project: High-Resolution paleoclimate records from the East African Rift System  
681 and their implications for understanding the environmental context of hominin evolution.  
682 *PaleoAnthropology* 2017:1–43.
- 683 9. Owen RB, Potts R, Behrensmeier AK, Ditchfield P (2008) Diatomaceous sediments and  
684 environmental change in the Pleistocene Olorgesailie Formation, southern Kenya Rift Valley.  
685 *Paleogeogr Paleoclimatol Palaeoecol* 269:17–37.
- 686 10. Behrensmeier AK, Potts R, Deino AL, Ditchfield P (2002) Olorgesailie, Kenya: a million  
687 years of hominin evolution.



681  
682  
683  
684  
685  
686  
687  
688  
689  
690  
691  
692  
693  
694  
695  
696  
697  
698  
699  
700  
701  
702  
703  
704  
705  
706  
707  
708  
709  
710  
711  
712  
713  
714  
715  
716  
717  
718  
719  
720  
721  
722  
723  
724  
725  
726  
727  
728  
729  
730  
731  
732  
733  
734  
735  
736  
737  
738  
739  
740  
741  
742  
743  
744  
745  
746  
747  
748

years in the life of a rift basin. *Spec Pub. SEPM* 73:97–106.

11. Behrensmeier AK, Potts R, Deino A (2018) The Oltulelei Formation of the southern Kenyan Rift Valley: A chronicle of rapid landscape transformation over the last 500 k.y. *Geol Soc Amer Bull* 130:1474–1492.

12. Brooks AS, Yellen JE, Potts R, Behrensmeier AK, Deino AL, Leslie DE, Ambrose SH, Ferguson JR, d'Errico F, Zipkin AM, Whittaker S, Post J, Veatch EG, Foecke K, Clark JB (2018) Long-distance stone transport and pigment use in the earliest Middle Stone Age. *Science* 360:90–94.

13. Deino AL, Behrensmeier AK, Brooks AS, Yellen JE, Sharp WD, Potts R (2018) Chronology of the Acheulean to Middle Stone Age transition in eastern Africa. *Science* 360:95–98.

14. Potts R, Behrensmeier AK, Faith JT, Tryon CA, Brooks AS, Yellen JE, Deino AL, Kinyanjui R, Clark JB, Haradon C, Levin NE, Meijer HJM, Veatch EG, Owen RB, Renaut RW (2018) Environmental dynamics during the onset of the Middle Stone Age in eastern Africa. *Science* 360:86–90.

15. Deino AL, King J, Heil C, Potts R, Behrensmeier AK, Dommain R (2016) *Chronology of the Olorgesailie Drilling Project Core 1A, Koora Graben, southern Kenya Rift*. Geol Soc Am Ann Meeting Denver 253-5.

16. Hublin J-J, Ben-Ncer A, Bailey SE, Freidline SE, Neubauer S, Skinner MM, Bergmann I, Le Cabec A, Benazzi S, Harvati K, Gunz P (2017) New fossils from Jebel Irhoud, Morocco and the pan-African origin of Homo sapiens. *Nature* 546:289–292.

17. Faith JT, Potts R, Plummer TW, Bishop LC, Marean CW, Tryon CA (2012) New perspectives on middle Pleistocene change in the large mammal faunas of East Africa: *Damalisca hypsodon* sp. nov. (Mammalia, Artiodactyla) from Lainyamok, Kenya. *Palaeogeogr Palaeoclimatol Palaeoecol* 361:64–93.

18. Eugster HP (1986) Lake Magadi, Kenya: a model for rift valley hydrochemistry and sedimentation? *Geol Soc Lond Spec Publ* 25:177–189.

19. Behr HJ (2002) Magadiite and magadi chert: a critical analysis of the silica sediments in the Lake Magadi Basin, Kenya. *Spec Publ SEPM* 73:257–273.

20. Hay RL, Sheppard RA (2001) Occurrence of zeolites in sedimentary rocks: An Overview, in: Natural Zeolites: Occurrence, Properties, Applications, eds Bish DL, Ming DW. *Min Soc Amer* 45:217–234.

21. Barker PA (1990) *Diatoms as paleolimnological indicators: a reconstruction of Late Quaternary environments in two East African salt lakes*, PhD thesis (Univ Loughborough, UK).

22. Barker P, Gasse F, Roberts N, Taieb M (1990) Taphonomy and diagenesis in diatom assemblages; a Late Pleistocene palaeoecological study from Lake Magadi, Kenya. *Hydrobiologia* 214:267–272.

23. Bonnefille R (1976) Implications of pollen assemblage from the Koobi Fora Formation, East Rudolf, Kenya. *Nature* 264:403–407.

24. Bonnefille R (2010) Cenozoic vegetation, climate changes and hominid evolution in tropical Africa. *Glob Planet Chang* 72:390–411.

25. Beentje HJ (1994) *Kenya trees, shrubs and lianas*. National Museums Kenya, Nairobi.

26. deMenocal P (2004) African climate change and faunal evolution during the Pliocene-Pleistocene. *Earth Planet Sci Lett* 220:3–24.

27. Jouzel J, Masson-Delmotte V, Cattani O, Dreyfus G, Falourd S, Hoffmann G, Minster B, Nouet J, Barnola JM, Chappellaz J, Fischer H, Gallet JC, Johnsen S, Leuenberger M, Loulergue L, Luthi D, Oerter H, Parrenin F, Raisbeck G, Raynaud D, Schilt A, Schwander J, Selmo E, Souchez R, Spahni R, Stauffer B, Steffensen JP, Stenni B, Stocker TF, Tison JL, Werner M, Wolff EW (2007) Orbital and Millennial Antarctic Climate Variability over the Past 800,000 Years. *Science* 317:793–796.

28. Candy I, Coope GR, Lee JR, Parfitt SA, Preece, R.C., Rose, J., Schreve, D.C., 2010. Pronounced warmth during early Middle Pleistocene interglacials: Investigating the Mid-Brunhes Event in the British terrestrial sequence. *Earth Sci Rev* 103:183–196.

29. Blain HA, Cuenca-Bescos G, Lozano-Fernandez I, Lopez-Garcia JM, Oille A, Rosell J, Rodriguez J (2012) Investigating the Mid-Brunhes Event in the Spanish terrestrial sequence. *Geology* 40:1051–1054.

30. Howard WRA (1997) Warm future in the past. *Nature* 388:418–419.

31. Levin NE (2015) Environment and climate of early human evolution. *Ann Rev Earth Planet Sci* 43:405–429.

32. Sikes N, Potts R, Behrensmeier A (1999) Early Pleistocene habitat in Member I Olorgesailie based on paleosol stable isotopes. *J Hum Evol* 37:721–746.

33. Scholz CA, Johnson TC, Cohen AS, King JW, Peck JA, Overpeck JT, Talbot MR, Brown ET, Kalinidekate L, Amoako PY, Lyons RP, Shanahan TM, Casteñada IS, Heil CW, Forman SL, McHargue LR, Beuning KR, Gomez J, Pierson J (2007) East African megadroughts between 135 and 75 thousand years ago and bearing on early-modern human origins. *Proc Nat Acad Sci* 104:16416–16421.

34. Ivory SJ, Blome MW, King JW, Mcglue MM, Cole JE, Cohen AS (2016) Environmental change explains cichlid adaptive radiation at Lake Malawi over the past 1.2 million years. *Proc Nat Acad Sci* 113:11895–11900.

35. Johnson TC, Werne JP, Brown ET, Abbott A, Berke M, Steinman BA, Halbur J, Contreras S, Grosshuesch S, Deino AL, Lyons RP, Scholz CA, Schouten S, Sinninghe Damsté JSA (2016) Progressively wetter climate in southern East Africa over the past 1.3 million years. *Nature* 537:220–224.

36. Ivory, S.J., Lézine, A.-M., Vincens, A., Cohen, A.S., 2018. Waxing and waning of forests: Late Quaternary biogeography of southeast Africa. *Glob Change Biol* 24:2939–2951.

37. Acosta VT, Schildgen TF, Clarke BA, Scherler D, Bookhagen B, Wittmann H, Blanckenburg von F, Strecker MR (2015) Effect of vegetation cover on millennial-scale landscape denudation rates in East Africa. *Lithosphere* 7:408–420.

38. Trauth M, Larrasoaña J, Mudelsee M (2009) Trends, rhythms and events in Plio-Pleistocene African climate. *Quat Sci Rev* 28:399–411.

39. Liu W, Martínón-Torres M, Cai Y-J, Xing S, Tong H-W, Pei S-W, Sier MJ, Wu X-H, Edwards RL, Cheng H, Li Y-Y, Yang X-X, Bermúdez de Castro JM, Wu X-J (2015) The earliest unequivocally modern humans in southern China. *Nature* 526:696–699.

40. Grün R, Stringer C, McDermott F, Nathan R, Porat N, Robertson S, Taylor L, Mortimer G, Eggins S, McCulloch M (2005) U-series and ESR analyses of bones and teeth relating to the human burials from Skhul. *J Hum Evol* 49:316–334.

41. Nielsen R, Akey JM, Jakobsson M, Pritchard JK, Tishkoff S, Willerslev E (2017) Tracing the peopling of the world through genomics. *Nature* 541:302–310.

42. Tierney JE, deMenocal PB, Zander PDA (2017) Climatic context for the out-of-Africa migration. *Geology* 45:1023–1026.

43. Scerri EML, Thomas MG, Manica A, Gunz P, Stock JT, Stringer C, Grove M, Groucutt HS, Timmermann A, Rightmire GP, d'Errico F, Tryon CA, Drake NA, Brooks AS, Dennell RW, Durbin R, Henn BM, Lee-Thorp J, deMenocal P, Petraglia MD, Thompson JC, Scally A, Chikhi L (2018) Did our species evolve in subdivided populations across Africa, and why does it matter? *Trends Ecol Evol* 8:582–594.

44. Potts R (1998) Variability selection in hominid evolution. *Evol Anthropol* 7:81–96.

45. Potts R (2007) Environmental hypotheses of Pliocene human evolution, in *Hominin environments in the East African Pliocene: an assessment of the faunal evidence*, eds Bobe R, Alemseged Z, Behrensmeier AK (Springer) pp 25–49.

46. Maslin MA, Trauth MH (2009) Plio-Pleistocene East African pulsed climate variability and its influence on early human evolution, in *The first humans - origin and early evolution of the genus Homo*, eds Grine FE, Fleagle JG, Leakey RE (Springer) pp 151–158.

47. Owen RB, Renaut RW, Behrensmeier AK, Potts R (2014) Quaternary geochemical stratigraphy of the Kedong-Olorgesailie section of the southern Kenya Rift. *Palaeogeogr Palaeoclimatol Palaeoecol* 396:194–212.

**Figures**

**Fig. 1. Core location and lithology.** a, Location of MAG14-2A and 1A and geology. b, Sediment log for MAG14-2A; c=clay, m = mud, si = silt, s = sand, e = evaporites.

**Fig. 2. Core chronology, geochemistry and mineralogy.** a, Geochemistry and mineralogy. LOI (550/1000) = Loss on Ignition and ignition temperatures (centigrade). Profile of Na/Ca ratios. Major authigenic minerals (excluding clays, quartz, feldspar) determined by X-ray diffraction. Minerals ordered to reflect generally higher salinities to the right. b, Bayesian chronological model. 1 = Excluded <sup>14</sup>C date that fails to follow a monotonic ordering. 2 = Excluded <sup>40</sup>Ar/<sup>39</sup>Ar date from a single crystal. Two chert dates from samples later found to contain secondary chalcocony were also excluded from the model. See SI for details.

**Fig. 3. Diatom-based environmental data.** Diatoms accumulated in a meromictic lake so separate conductivity and pH transfer functions are shown for mixed, saline and fresh water taxa. Habitats indicated separately for saline and fresh taxa.

**Fig. 4. Pollen stratigraphy.** Selected taxa shown. Pollen PCA 1 summarizes all pollen data and shows a long-term reduction in PCA values from ~575 ka that reflects increased aridity. Poaceae increase upwards with Cyperaceae and *Podocarpus* declining. Other taxa suggest increasing aridity during the last half million years.

**Figure 5. Temporal environmental change in the Magadi basin and regional comparisons.** Major hominin/faunal events in eastern Africa (except where noted) to left (8). First appearance of *H. sapiens* in Africa from Morocco data (16). *H. sapiens* dispersal: 1 = genetic data (41), 2 = fossil data (39, 40). FAD = First Appearance Datum; LAD = Last Appearance Datum. Thick dashed line shows the Mid-Brunhes Event (MBE). a, Na/Ca ratios. Decline reflects change from fresh to saline alkaline lake. b, Pollen PCA 1. Low values reflect increased aridity. c, Poaceae to aquatic pollen ratios (P-A/P+A). High values indicate wetter episodes. d, Diatom Principal Component Analysis. High values reflect benthic taxa introduced to a meromictic lake by flooding. Note that many of these flood events broadly correlate (diagonal shading) with interglacial episodes in "g". e, Insolation (1°S) from AnalySeries 2.0. High variability periods shaded. f, Northwest Indian Ocean dust record (26). Note long-term increasing aridity through the last 400 ka. g, Change in deuterium in Vostok ice core, East Antarctica (27). Note increased variability in glacial-interglacial cycles after the MBE. h, Diatom-inferred environmental change, Olorgesailie Basin (47).

749  
750  
751  
752  
753  
754  
755  
756  
757  
758  
759  
760  
761  
762  
763  
764  
765  
766  
767  
768  
769  
770  
771  
772  
773  
774  
775  
776  
777  
778  
779  
780  
781  
782  
783  
784  
785  
786  
787  
788  
789  
790  
791  
792  
793  
794  
795  
796  
797  
798  
799  
800  
801  
802  
803  
804  
805  
806  
807  
808  
809  
810  
811  
812  
813  
814  
815  
816